Spectroscopy of the Mirror Instability Growth Rate in Hollow Electrodes Discharge (HED) Plasma

Murad M. Kadhim[1*], Qusay A. Abbas[2]

Abstract

In this work, an experimental study was conducted about the effect of gas pressure on the growth rate of the mirror instability produced in hollow electrodes discharge (HED) plasma in two regions: inter-electrodes gap and internal cathode cavity, by optical emission spectroscopy. Optical emission spectroscopy measurements, at different gas pressures in two regions under study, show that the electron number density (n_e) increase with increasing gas pressure from 0.04 to 0.2 Torr. While the electron temperature (T_e) decrease with increased gas pressure. In addition, the growth rate increase with increasing electron temperature anisotropy in both regions.

Key Words: Hollow Electrodes Discharge (HED), Mirror Instability, Optical Emission Spectroscopy (OES), Electron Temperature (T_e), Electron Number Density (n_e).

DOI Number: 10.14704/nq.2021.19.11.NQ21182 **NeuroQuantology 2021; 19(11):116-125**

Introduction

The distribution of plasma and the model that can be described largely depends on the shape and size of the electrodes used (especially the cathode), one relative to the other (Al-Hakary et al., 2014). The discharge is characterized by maximum ion density and a bright plasma in the small anode region. Since the anode area in these plasma sources is small enough compared to the cathode area, it has been called the narrow anode plasma source (Miljevic, 2002). Many different forms of cathodes are known as hollow cathodes. All hollow cathodes are thermionic devices that depend on the ionization of a neutral gas by electron bombardment to generate plasma (Domonkos, 1999). Hollow cathode discharge (HCD) can produce dense plasma and has been used to develop high-rate processing machines with high efficiency and low pressure (Zhechev et al, 2003). The engineering feature of HCD enhances the oscillations of hot electrons within the cathode, thus improving ionization, ion bombardment of the inner walls, and other subsequent processes. With the same strength, the hollow cathode shows the plasma density one or two times higher than the conventional flat electrodes (Al-Hakary, 2013).

In order to determine plasma parameters such as electron temperature (T_e), electron number density (n_e), Debye length (λ_D), and plasma frequency (ω_{pe}), optical emission spectroscopy (OES) has been used. The Boltzmann plot method is a simple and widely used for spectroscopic measurement, especially for measuring the T_e (Arshad et al., 2016). Boltzmann distribution is satisfied in case of local thermodynamic equilibrium (Conrads and Schmidt, 2000).

$$\mathrm{Ln}(\lambda_{mn} I_{mn}/hc\, g_m A_{mn}) = -E_m/kT_e + \mathrm{Ln}(N/U) \quad (1)$$

Corresponding author: Murad M. Kadhim
Address: [1*]University of Baghdad, Baghdad, Iraq; [2]University of Baghdad, Baghdad, Iraq.
[1*]E-mail: murad.kadhim1204@sc.uobaghdad.edu.iq
Relevant conflicts of interest/financial disclosures: The authors declare that the research was conducted in the absence of any commercial or financial relationships that could be construed as a potential conflict of interest.
Received: 11 September 2021 **Accepted:** 19 October 2021

Where: I_{mn}, λ_{mn} and A_{mn} are the intensity, wavelength and transition probability correspond to transition from m to n, g_m is a statistical weight, h is the Planck's constant, N is the number density of emitting species, c is the speed of light, U is partition function.

The Stark broadening effect was used to calculate the n_e requires a line which is free from self-absorption (Llewellyn, 1957):

$$n_e(cm^{-3}) = [\Delta\lambda/2\omega_s]\, N_r \quad (2)$$

Where as, $\Delta\lambda$ is the full width at half maximum of the line, and ω_s is the theoretical line full-width Stark broadening parameter, which calculated at the same reference electron density $N_r = 10^{16}(cm^{-3})$.

One of the important plasma parameters β, which is the ratio between the plasma thermal pressure (kinetic energy) to the magnetic field pressure (magnetic energy) is also analytically evaluated (Raju et al, 2014):

β = Particle or thermal pressure/ Magnetic field pressure

$$\beta = \frac{n_e k_B T_e}{\frac{B^2}{2\mu_0}} \quad (3)$$

Since $B^2/2\mu_0$ is the magnetic field pressure.

Mirror instability occurs in the case of anisotropic plasma pressure in the presence of magnetic fields. The electron temperature anisotropy (A_e) can enhance the mirror instability growth rate, leads to the generation of plasma instabilities.

The electron temperature anisotropy is defined as (Kivelson and Southwood, 1996):

$$A_e = T_{e\perp}/T_{e\parallel} \quad (4)$$

The $T_{e\perp}$ is the perpendicular electron temperature with respect to the background magnetic field. While $T_{e\parallel}$ is the parallel electron temperature to the magnetic field lines (i.e. it represents the electron temperature at the highest pressure). For the given plasma parameters, the maximum growth rate of the electron mirror instability is (Kivelson and Southwood, 1996).

$$\gamma_{me} = \omega_{ce}\sqrt{(v_{e\perp}^2/c^2) + 1} \quad (5)$$

Where: γ_{me}, ω_{ce}. c and $v_\perp$ are the maximum growth rate, cyclotron frequency, the speed of light and the perpendicular electron temperature to the magnetic field lines, respectively.

In this work, we have studied the influence of growth rate on plasma characteristics produced by DC discharge in Argon gas in hollow electrodes system. That is, the hollow electrodes represent both the hollow cathode and anode.

Experimental Part

Figure (1) illustrated the DC hollow electrodes discharges (HED) chamber that used in this work. The vacuum chamber is made from cylindrical Pyrex glass with a length of 37cm and diameter 30cm. Two small pipes connected in mid-top and bottom of the chamber, one of them was linked to pumping systems, while the other was used to supply the Argon gas (99.9% purity). The chamber was evacuated by two stages rotary pump, CIT-ALCATEL Annecy, (made in France) to a base pressure 2×10^{-2} Torr. One permanent magnet which has a value of 3.4mT was used to confinement of plasma located behind the cathode electrode which measured by a digital teslameter made by Brolight Company, Model: BEM-5032, (made in China). Digital Pirani gauge type Edward, (made in England) was used to measure the pressure of the chamber from atmospheric to the base pressure of the vacuum system. The hollow electrodes usually have a cylindrical geometry which made from aluminum with an inner diameter and inner length is 6 and 3cm, respectively. Both electrodes are fixed by Teflon to prevent any connection with the chamber walls; and the distance between the two electrodes is 8cm. The working principle of this device is the glow discharge between the electrodes. In this device, the normal glow discharge is produced when a DC constant voltage of about 4kV is applied between the two electrodes. Due to this external voltage, the argon plasma discharge is formed and then the voltage of the electrodes will drop. The emission spectrum that emitted from the plasma is detected by the Optical emission spectrometer model Thorlabs (made in Germany) to determine plasma characteristics by diagnostics of the spatially integrated plasma light emissions for a wavelength range of 320-740nm. The spectrometer was placed at the angle of 45^0 from the plasma column. The results of the spectrum of this system were calibrated with NIST database software to calculate the plasma characteristics in two regions: inter-electrodes gap and internal cathode cavity.

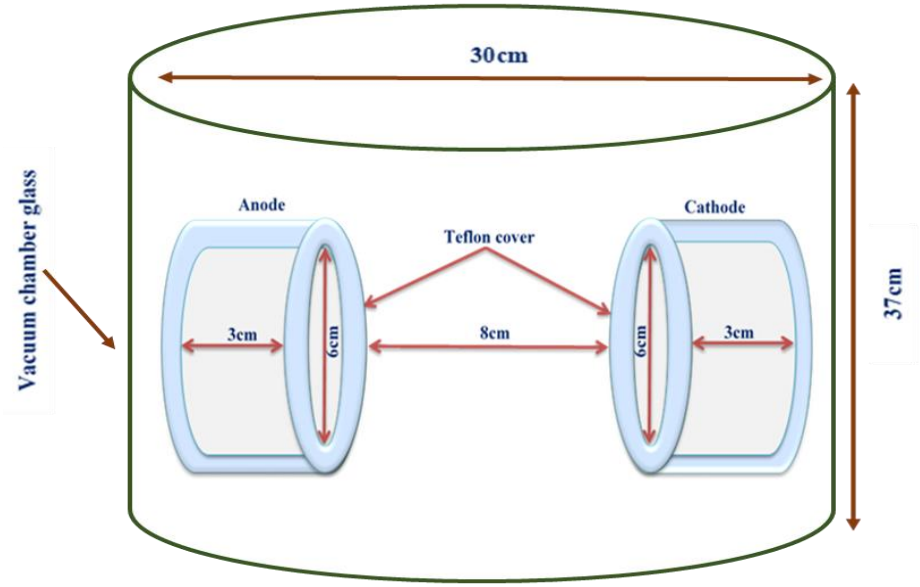

Figure 1. Schematic of the hollow electrodes discharge chamber

Results and Discussion

Figure (2) demonstrated the influence of gas pressure on the normal glow discharge (NGD) regions of hollow electrodes discharge (HED) system in two groups: A) Internal cathode cavity and B) Inter-electrodes gap. It is pointed out from the figure that the cathode and anode fall are confined in the inter electrodes cavities and both fall regions are compressed, the negative glow becomes a thin layer of intense luminosity, while the positive column increased. This result agrees with the reference (Klagge and Lunk, 1991). The presence of the mirror configuration causes both electrodes fall to be more compressed and the negative glow thinner with higher intensity. This result agrees with the reference (He et al, 2011).

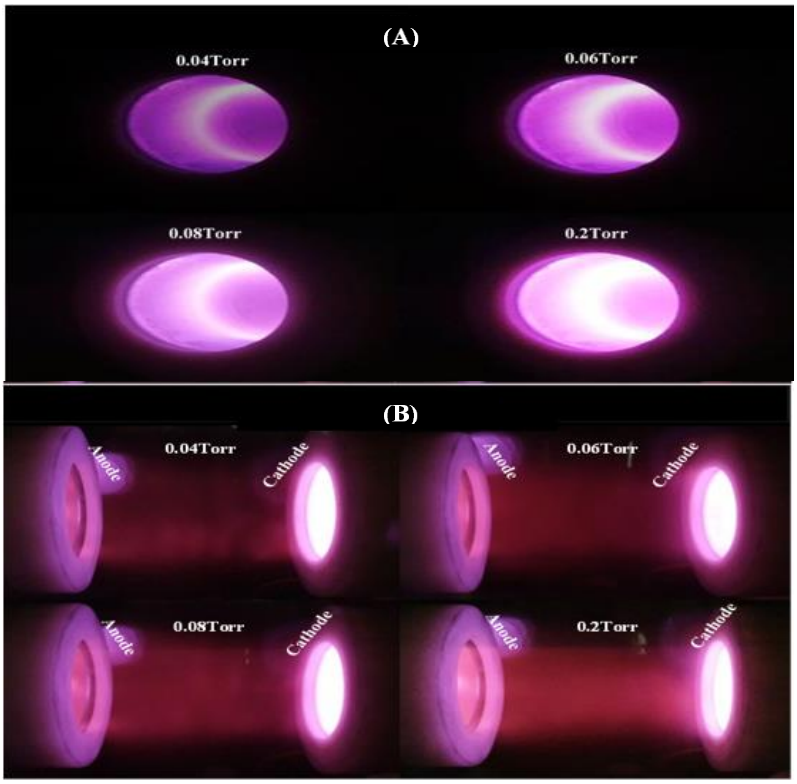

Figure 2. The influence of gas pressure on the normal glow discharge regions, in two groups: A) Internal cathode cavity and B) Inter-electrodes gap.

Figure (3) shows the influence of the gas pressure on the I-V curves in hollow electrodes discharge (HED) system. The I-V curve was specifically split into two regions (I and II regions). In low discharge current (region I), the pre-discharge appears and has a positive resistance. In this region, the discharge takes place mostly outside of the electrode cavity (between the outer surface of the cathode and the anode). In this range of currents, the behavior of the I-V characteristic, as well as the configuration of the discharge, resembles that of a parallel-plate discharge. While in region II, with constant voltage and increasing current, the normal glow discharge was created. The discharge switches to a model like normal glow discharge between parallel electrodes as the current increases and the I-V characteristic becomes planar. The discharge continues to work both inside the cavity and from the cathode's outer surface as the emission more intense. Simultaneously, the discharge becomes greatly constrained, and it primarily operates inside the cavity. The transition to a more "effective" regime characteristic of the "hollow cathode effect" is indicated by a significant increase in current density accompanied by a decrease in voltage. This result agrees with the reference (Pessoa et al, 2007). The data illustrated that I-V curves decreased with increasing gas pressure from 0.04 to 0.2, due to plasma confinement in a strong electric field region (inside the electrodes cavities) (Hassouba and Dawood, 2011).

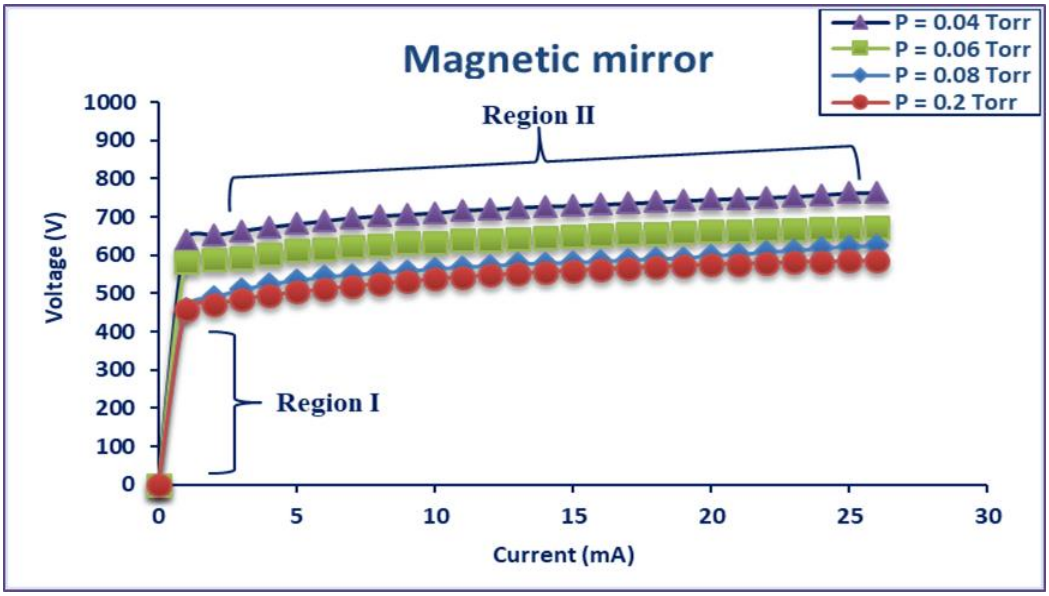

Figure 3. I-V curves of Argon gas for HED, with magnetic mirror.

The emission spectrum that is emitted from the Ar plasma are detected by optical emission spectrometer to determine plasma characteristics by diagnostics of the spatially integrated plasma light emissions for a wavelength range of 320-740nm. The spectrometer was placed at the center of the plasma column. The results of the spectrum of this system were calibrated with NIST database software to calculate the plasma characteristics. The emission spectrum of Ar plasma in hollow electrodes system at different gas pressures (0.04, 0.06, 0.08 and 0.2Torr) in two regions: A) internal cathode cavity and B) inter-electrodes gap, are shown in figure (4). One can observe from this figure that there are many peaks of the argon neutral atom (Ar I) lines that appear at the wavelengths 337.347, 389.466, 427.217, 476.867, 603.213, 675.283, 697.028, 706.874, 715.884 and 735.081nm in this spectrum. The ionic emission lines of Ar II were also detected at the wavelengths 357.69 and 654.48nm. All peaks intensity increasing with increasing gas pressure from 0.04 to 0.2 Torr (with a higher rate in the internal cathode cavity compare with the inter-electrodes gap), due to increasing the electron number density hence increase the collision's probability between the electrons and gas atoms, which allows electrons to have enough excitation energy. This result agrees with the reference (Bellan, 2006).

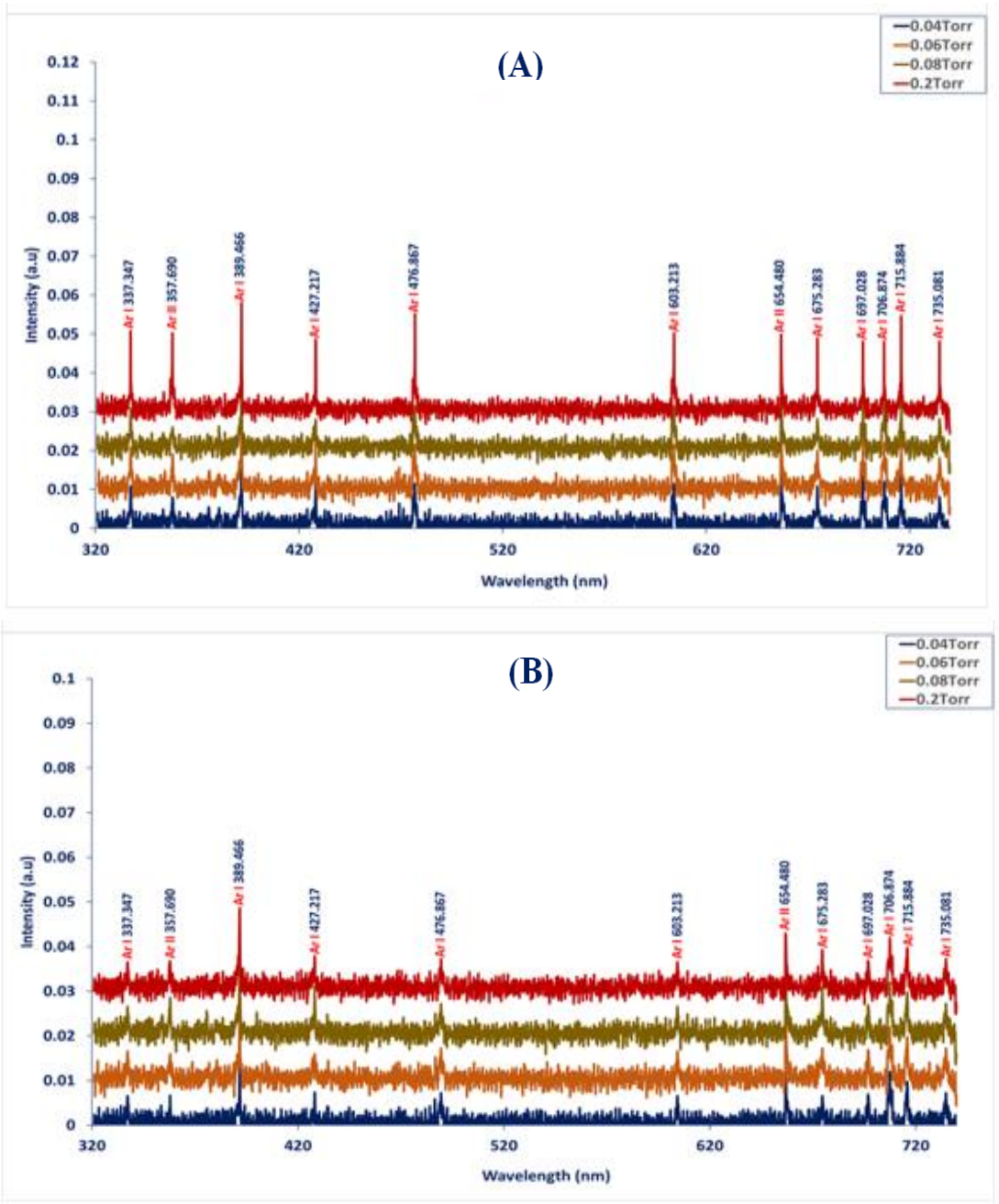

Figure 4. The optical emission spectra of Ar plasma at different gas pressures, in two regions: A) internal cathode cavity and B) inter-electrodes gap, in the magnetic mirror

The value of T_e was calculated according to the Boltzmann plot method (equation (1)) with data listed in the table (1) (Park et al, 2010).

Table 1. Ar I standard lines are used to calculate electron temperature, and their characteristics (NIST, 2020).

λ(nm)	$A_{ji} \times g_i$	E_i(eV)	E_j(eV)
361.586	13×10^5	20.939965	24.367883
546.258	333×10^5	21.152682	23.421752
596.091	38.7×10^5	21.159916	23.239296
630.925	0.855×10^5	21.159916	23.124489

Figures (5) and (6) show the Boltzmann plot method using the selected atomic argon lines (ArI) for the hollow electrodes discharge system, in cases under study at different gas pressures.

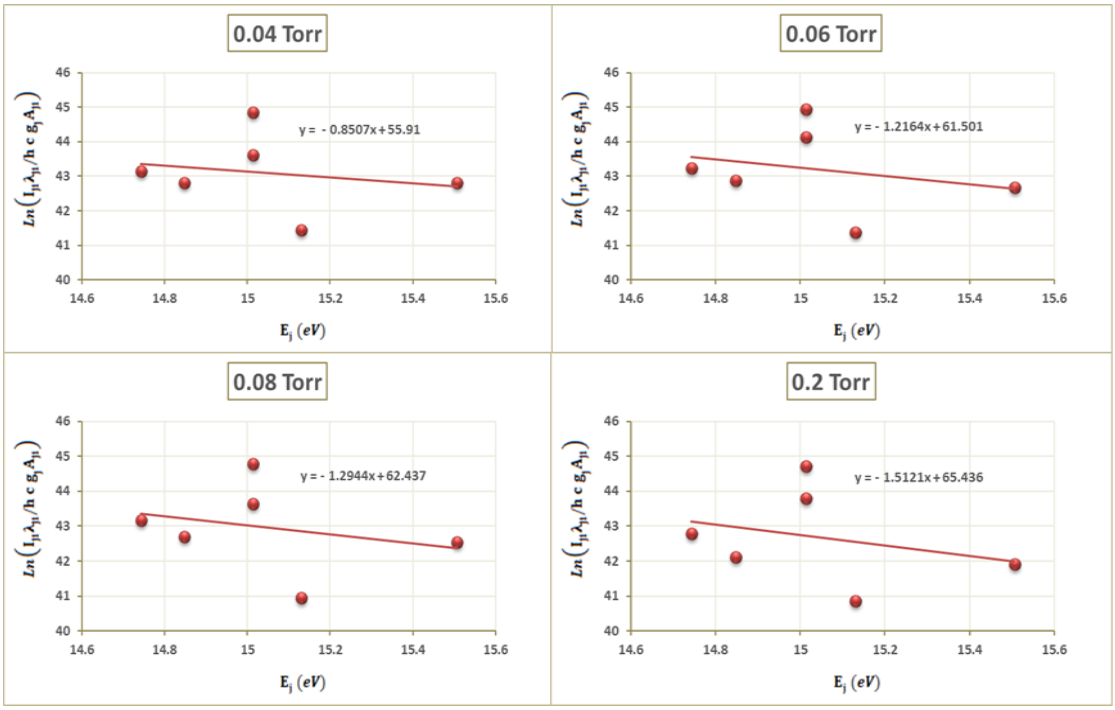

Figure 5. Boltzmann plot for ArI peaks using the hollow electrodes system at different gas pressures, in the inter-electrodes gap

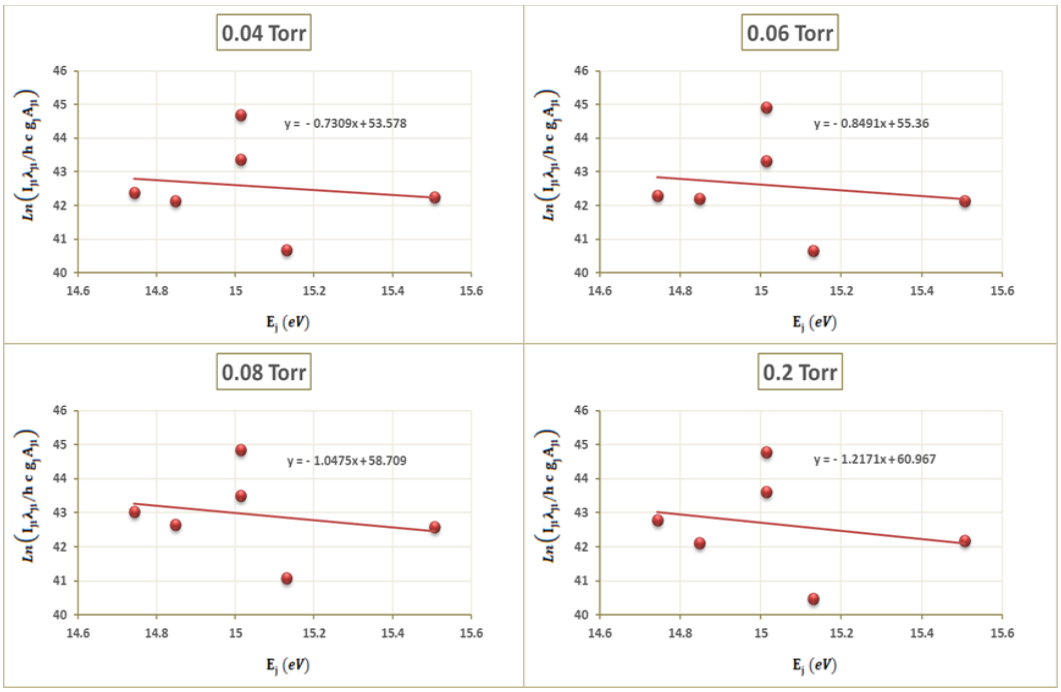

Figure 6. Boltzmann plot for ArI peaks using the hollow electrodes system at different gas pressures, in the internal cathode cavity

Figure (7) represents the effect of the gas pressure on the behavior of the T_e in two regions: inter-electrodes gap and internal cathode cavity. The data detected the T_e decreased with the increase of gas pressure from 0.04 to 0.2 Torr in both regions. As a result of the transfer of electron energy to the gas atoms, the gas temperature increases while the T_e and the average kinetic energy of the electron decreased. In addition, in the internal cathode cavity the electron temperature was increased compared to its value in the inter-electrodes gap. Due to confine the plasma in the region of a strong electric field, this confinement causes an energy of the electrons. This result agrees with the reference (Park et al, 2010).

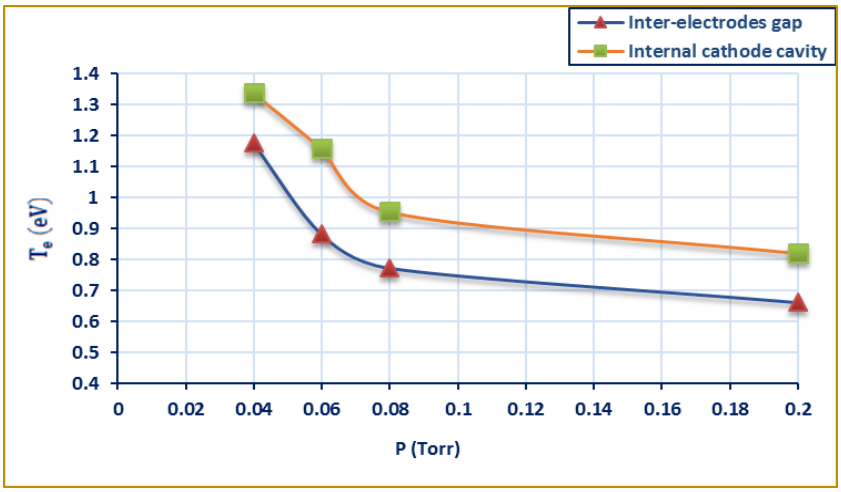

Figure 7. The variation of $\mathbf{T_e}$ against the gas pressure in two regions: inter-electrodes gap and internal cathode cavity

n_e can be calculated by using equation (2), which is called the Stark broadening effect depending on the standard values of broadening for this line ($N_r = 10^{16}cm^{-3}$) (Konjevic et al, 1990). Figure (8) illustrated the influence of the gas pressure on the behavior of electron number density in two regions: inter-electrodes gap and internal cathode cavity. One can observe that the electron number density increases with the increase of gas pressure in two regions. The increasing of gas pressure will lead to increasing inelastic collisions between electrons and Ar atoms and hence increasing the electron number density. This result agrees with the reference (Hassouba, 2001). As well as, the magnetic mirror configuration causes the plasma to be confined in a small volume (with a higher rate in the internal cathode cavity compare with the inter-electrodes gap), which leads to a further increase in the n_e. This result agrees with the reference (Post, 2002).

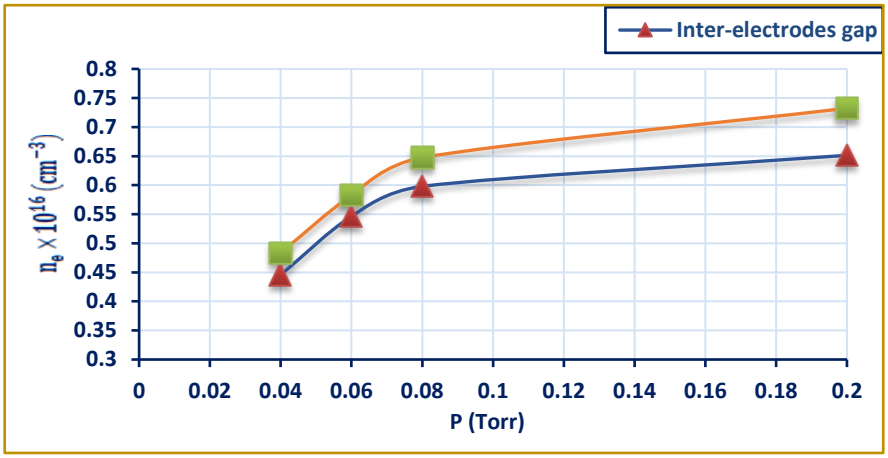

Figure 8. The difference of $\mathbf{n_e}$ against the gas pressure in two regions: inter-electrodes gap and internal cathode cavity

Table (2) shows the calculated values of n_e and T_e for DC discharge plasma in Argon at different working pressures, in two regions: inter-electrodes gap and internal cathode cavity. In general, the values of n_e and T_e in the internal cathode cavity higher than their values in the inter-electrodes gap due to plasma confinement (Langmuir, 1929).

Table 2. Plasma parameters for hollow electrodes discharge (HED) system

Plasma Region	P (Torr)	T_e (eV)	$n_e \times 10^{16}$ (cm^{-3})
Inter-electrodes gap	0.04	1.1755	0.4457
	0.06	0.8821	0.5462
	0.08	0.7726	0.5979
	0.2	0.6613	0.6513
Internal cathode cavity	0.04	1.3382	0.4836
	0.06	1.1577	0.5824
	0.08	0.9547	0.6474
	0.2	0.8216	0.7323

According to equation (3), the influence of work pressure on the value of β is calculated and plotted in figure (9). Many features can be obtained; the β-value has a non-uniform profile between hollow electrodes. The β-values were less than unity in the electrode distance separation. This result means that this electrode configuration has good plasma confinement compare with the other electrode configurations. In addition, the value of beta decreases with the increase in gas pressure due to the decrease in plasma temperature. This result agrees with reference (Brunel, 1993).

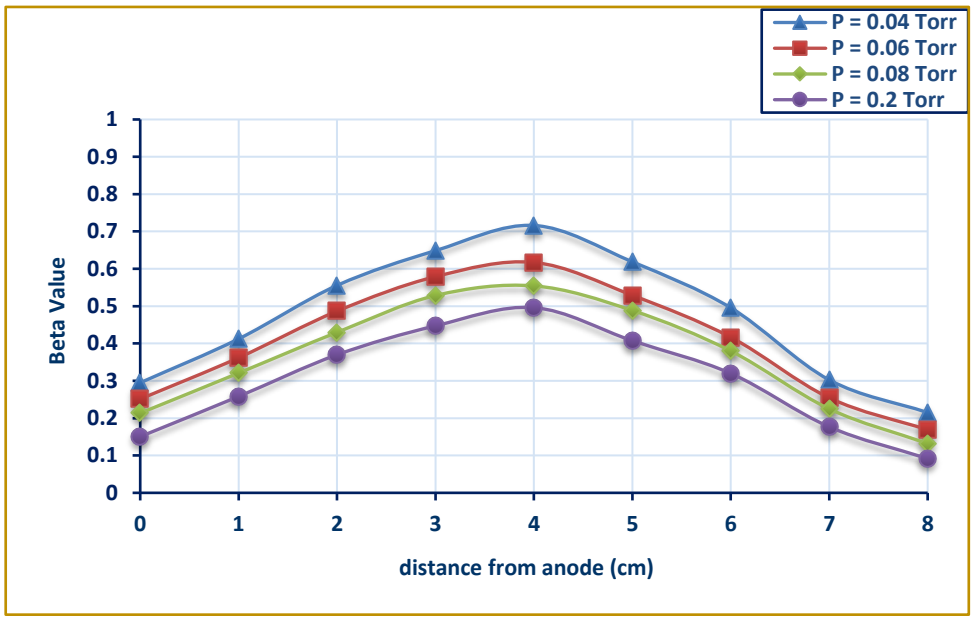

Figure 9. The variation of β-value with the distance from anode for the inter-electrodes gap at different gas pressures

The growth rate of the mirror instability is measured according to equation (5) and draw in figure (10). This figure illustrated the growth rate of the mirror instability as a function of electron temperature anisotropy (A_e) in two regions: inter-electrodes gap and internal cathode cavity. The data detected was the increasing instability growth rate with increasing electron temperature anisotropy in both regions. And this is due to the particle pressure generated by the magnetic confinement (i.e. increasing in β-value) with increasing electron temperature anisotropy. This result agrees with the reference (Pitcher and Stangeby, 1997). In addition, the mirror instability in the internal cathode cavity has a larger growth rate compared to the inter-electrodes gap. Because of the pendulum effect, where an electron oscillates back and forth, creating secondary electrons, therefore the growth rate boosts in the internal cathode cavity. This result agrees with the reference (Ahmadi et al, 2016).

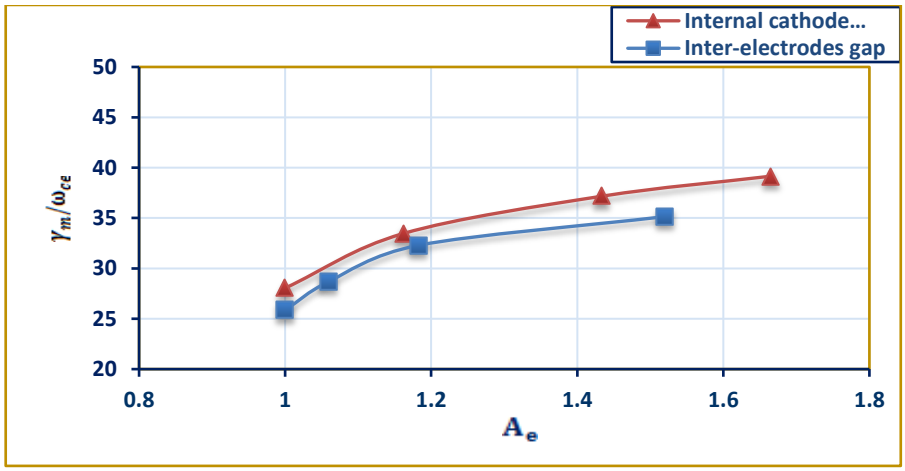

Figure 10. The growth rate as a function of electron temperature anisotropy

Furthermore, figure (11) represented the variation of the growth rate with gas pressure in the two regions under study. The data detected the growth rate was decreased with the working pressure increases in both regions with a different rate. The hollow cathode effect which responsible for the pendulum movement of electrons in the cathode cavity causes enhances growth instability in the internal cathode cavity. This result agrees with the reference (Hasegawa, 1975).

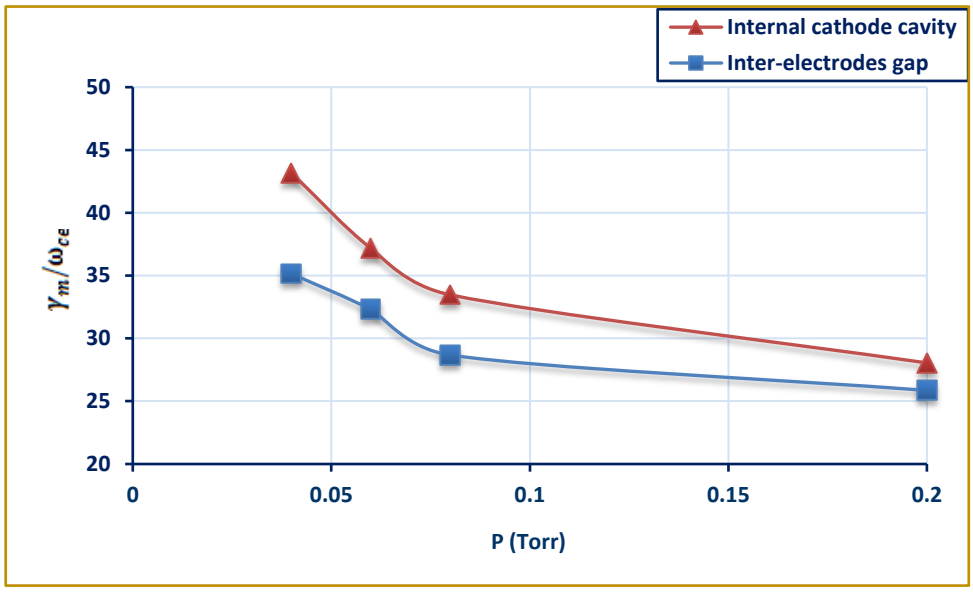

Figure 11. The growth rate as a function of gas pressure

Conclusion

In summary, the I-V curves decreased with increasing gas pressure from 0.04 to 0.2 in hollow electrodes discharge (HED) system. Plasma characteristics like electron temperature (T_e) decrease with increasing gas pressure, while the electron number density (n_e) increases with increasing gas pressure. The values of T_e and n_e in the internal cathode cavity higher than their values in the inter-electrodes gap. In addition, the effect of the magnetic mirror configuration was observed in the boosts the confinement of plasma through the measurement of beta value, its value is less than 1. The measured beta value decreases with increasing gas pressure. The growth rate increase with increasing electron temperature anisotropy in regions under study, but at a higher rate in the internal cathode cavity.

References

Al-Hakary SK, Dosky L, Talal SK. Investigation of Hot Cathode and Hollow Anode of Argon Glow Discharge Plasma. *Applied physics research* 2014; 6(5): 45-56.

Miljevic V. Cylindrical hollow anode ion source. *Review of scientific instruments* 2002; 73(2): 751-753.

Domonkos MT. Evaluation of Low-Current Orificed Hollow Cathodes. PhD thesis, University of Michigan 1999.

Zhechev D, Zhemenik VI, Tileva S, Mishinsky GV, Pyrvanova N. A hollow cathode discharge modification as a source of sputtered atoms and their ions. *Nuclear Instruments and Methods in Physics Research Section B: Beam Interactions with Materials and Atoms* 2003; 204: 387-391.

AL-Hakary SK, Amedi AFA, Dosky LM. Theoretical and Experimental Investigation of Hollow Cathode Nitrogen Glow Discharge Plasma. *International Journal of Engineering Research and Development* 2013; 7(2): 10–17.

Arshad A, Bashir S, Hayat A, Akram M, Khalid A, Yaseen N, Ahmad QS. Effect of magnetic field on laser-induced breakdown spectroscopy of graphite plasma. *Applied Physics B* 2016; 122(3).

Conrads H, Schmidt M. Plasma generation and plasma sources. *Plasma Sources Science and Technology* 2000; 9(4): 441-454.

Llewellyn JF. Ionization and Break down in Gases. New York: John Wiley & Sons Inc 1957.

Raju MS, Singh RK, Gopinath P, Kumar A. Influence of magnetic field on laser-produced barium plasmas: Spectral and dynamic behaviour of neutral and ionic species. *Journal of Applied Physics* 2014; 116(15).

Kivelson MG, Southwood DJ. Mirror instability II: The mechanism of nonlinear saturation. *Journal of Geophysical Research: Space Physics* 1996; 101(A8): 17365-17371.

Klagge S, Lunk A. Probe diagnostics of anisotropic plasma in a hollow cathode arc. *Journal of applied physics* 1991; 70(1): 99-105.

He SJ, He F, Li S, Ouyang JT. Spectroscopic diagnosis of striation in hollow cathode discharge. *Guang pu xue yu Guang pu fen xi= Guang pu* 2011; 31(3): 608-611.

Pessoa RS, Sismanoglu BN, Amorim J, Petraconi G, Maciel H. Hollow cathode discharges: low and high-pressure

operation. *Gas Discharges, Fundamentals and Applications* 2007; 27(5): 176-190.

Hassouba MA, Dawood N. Study the effect of the magnetic field on the electrical characteristics of the glow discharge. *Advances in Applied Science Research* 2011; 2(4): 123-131.

Bellan PM. Fundamental of plasma physics. Cambridge University Pressm 2006.

Park H, You SJ, Choe W. Correlation between excitation temperature and electron temperature with two groups of electron energy distributions. *Physics of Plasmas* 2010: 17(10).

NIST (2020). https:// www.nist.gov/pml/atomic-spectra-database.

Konjevic N, Lesage A, Fuhr J, Wiese, W. Experimental Stark widths and shifts for spectral lines of neutral and ionized atoms. *Journal of Physical and Chemical Reference Data* 1990; 19(2): 1307–1385.

Hassouba MA. Effect of the magnetic field on the plasma parameters in the cathode fall region of the DC-glow discharge. *The European Physical Journal Applied Physics* 2001; 14(2): 131-135.

Post RF. Open and Closed Magnetic Confinement Systems: Is There a Fundamental Difference in Their Transport Properties. *Review Literature and Arts of the Americas* 2002; 11(4): 345-360.

Langmuir I. The Interaction of Electron and Positive Ion Space Charges in Cathode Sheaths. *Physical Review* 1929; 33(6): 954-989.

Brunel F, Tajima T. Confinement of a high-beta plasma column. *The Physics of Fluids* 1983; 26(2): 535-544.

Pitcher CS, Stangeby PC. Experimental divertor physics. *Plasma Physics and Controlled Fusion* 1997; 39(6): 779-730

Ahmadi N, Germaschewski K, Raeder J. Effects of electron temperature anisotropy on proton mirror instability evolution. *Journal of Geophysical Research: Space Physics* 2016; 121(6): 5350-5365.

Hasegawa A. *Plasma instabilities and nonlinear effects.* Berlin, New York, Springer-Verlag 1975.

Khalaf AJ, Hasan NB. Investigation and prepared of Cu_2ZnSnS_4 compound films as a gas sensor by pulse laser deposition. *NeuroQuantology* 2020; 18(1): 117-123.